EMAS Engineering Modelling, Analysis & Simulation THE NAFEMS JOURNAL

NAFEMS

Vol. 2, Issue 1, 2025

Experimental and Numerical Approaches to Optimize Heat Blocking Efficiency in Intumescent Coatings

Taher Hafiz[a,1], James Covello[a], Gary Wnek[a], Ya-Ting Liao[b], Edrissa Gassama[c], Abdul Kareem Melaiye[d]

[a]Macromolecular Science and Engineering, Case Western Reserve University, Cleveland, 44106 OH USA,
[b]Mechanical and Aerospace Engineering Case Western Reserve University, 44106 OH USA,
[c]Equity Engineering Group, Research and Development, Shaker Heights, 44122 OH USA,
[d]Goodyear Tire & Rubber Company, Research and Development, Akron, 44316 OH USA.

Abstract

Intumescent coatings, which swell and form a protective char when exposed to flame, are key for fire protection. This study evaluates the Heat Blocking Efficiency (HBE) of epoxy resin coatings, incorporating eco-friendly tannic acid (TA) and ammonium polyphosphate (APP) on hot-rolled carbon steel (HRCS). Using a methane torch, a 6.3-mm thick HRCS plate was subjected to 130 kW/m^2 heat flux. To predict heat transfer and estimate HBE, we combined experimental methods and numerical simulations involving a two-dimensional heat conduction model via finite element analysis (FEA), considering thermal insulation, heat flux boundary conditions, convection, and radiation. The results aligned closely with experimental data, confirming the coatings' efficacy in keeping steel temperature below the critical range of 550-600°C for up to 20 minutes, with the minimum temperature observed under 250°C. The coatings' HBE successfully reduced the substrate temperature by 90%, demonstrating their potential for advancing fire safety in coatings technology.

Keywords

Intumescent Coating, Protective Layer, Heat Blocking Efficiency, Heat Transfer

1 Introduction

For the last five decades, increasing attention has been given to the intumescent coating for protecting structural carbon steel from the motion of fire. The application of a flame-retardant coating has been the focus of development in fire safety. Fire events are common and dangerous, so we should have high-tech prevention methods. Understanding how intumescent coatings work and finding applications for them are the dreams of ongoing research and development in fire safety engineering. As the world burns with more significant and hotter flames, there is no choice but to research light-resisting coatings A comprehensive primary study was conducted on flame-retardant coatings to explore the mechanisms by which intumescent coatings suppress fire and how they can be applied in practice [1]-[3]. Besides increasing safety, computer-generated fire simulation also helps to generate new ideas. This type of research gives us a more proactive attitude toward reducing fire risk [4].

An intumescent coating is an inactive fire safety that expands when exposed to high temperatures. The expansion forms an insulating barrier to protect structural steel from severe heat [5], [6]. The effectiveness of intumescent coating is affected by its chemical composition, which generally contains a mixture of an acid source, which decomposes to form mineral acid [7],[8]; a carbon source that dehydrates to build a char [9] a blowing agent releases non-combustible gases forming a foam-like char

[1]Corresponding author.
E-mail address: tbh25@case.edu (T. Hafiz)
https://doi.org/10.59972/xny38fpw

layer; and a binder which acts as a medium, upon exposure to heat to form a solid protective barrier [10]. These actions slow the heat transfer rate to the underlying metal substrate and increase the heat-blocking efficiency of the coating [11], [12]. The growth of intumescent coating and the Heat blocking efficiency (HBE) depends on several factors, including but not limited to thermal conductivity [13], specific heat capacity, density, emissivity, initial application thickness [14], and the intensity of the heat source [15].

Numerous approaches have been explored in the literature to simulate the behaviour of intumescent coatings. Computational models such as finite element analysis (FEA) [16] and computational fluid dynamics (CFD) [17] have been developed to predict the intumescent layer, thermal growth, and performance under fire conditions. However, accurately capturing (HBE) and modelling the transition from a liquid to a solid into an expanded foam remains challenging. Further research is necessary to validate these models using analytical solution techniques and/or to validate them against experimental data for diverse intumescent formulations and fire scenarios. Cirpici et al. [18] investigated the performance of intumescent coating on a concrete column under different fire conditions. In another paper, Cirpici et al. [18]-[13] investigated the effect of coating and substrate parameters on the intumescent coating expansion and effective thermal conductivity. Kang et al. [19] determined the heat-blocking efficacy in their experiment. Other researchers have also conducted experiments to calculate the apparent thermal conductivity of intumescent coatings on steel plates [19]-[21]. Zhang et al. [22] were among the first to analyse the behaviour of intumescent layers on steel under varying heating conditions, and they achieved an excellent agreement between numerical simulations and experimental observations.

Current studies in fire retardants using finite element analysis (FEA) have focused on the heat transfer, thermal response of materials, and the development of predictive models for fire in complex geometries. For instance, M. Rusthi et al. [23] validate the accuracy of finite element methods and simulate the fire performance of steel frame walls using 3-D heat transfer models. The author validated his model by comparing his results with the results from fire tests conducted on various non-load bearing and load bearing wall systems under different load conditions. However, the assumptions he made to represent connections may only partially reflect actual physical conditions, which could impact the accuracy of his predictions. Huang et al. [24] used analytical solution to validated the modelling and simulation accuracy of his modelling and Burak et al. [25] conducted a validation study based on comparing against Eurocode-EN 1993-102 whereas Burkhart et al. [26] present a framework validation and verification of computational models when developing and utilizing finite element models for heat transfer application.

Experimental approaches, Laboratory testing methods are essential in providing valuable data necessary for validating and confirming computational predictions. The Fire Safety Research Institute has contributed to validating computational fire models using the Fire Dynamics Simulator (FDS) [27] to predict the intumescent coating performance during laboratory gas burner experiments [28]. National Fire Research Laboratory (NFRL) setup and conducted real scale fire experiment to evaluate thermal protection performance and to validate physics-based predictive models [29], [30]. The National Institute of Standards and Technology (NIST) has also been involved in developing laboratory-scale testing of intumescent coating for fire safety [31], [32].

Burak et al. [25] were among many researchers who used numerical simulation to modelled the heat transfer through thin film intumescent coating. He also made a comparison study of steel temperature under ISO 834 by assuming constant thermal conductivity. In another study [33], a cone heater was used to understand the heat transfer through an object and to measure the expansion process of intumescent coatings on steel plates coated with three different thicknesses of the coating. Mauro et al. examined the thermal response of intumescent coatings using a blowtorch as a heat source to simulate exposure scenarios [34].

Despite these studies, the literature still needs to include a complete investigation of the heat-blocking efficiency and fire performance of steel elements protected by intumescent coatings with varying chemical compositions. The above numerical model's accuracy in predicting the heat blocking efficiency and the behaviour of intumescent coating is not fully established. In this work, the numerical simulations and experiment measurements will be used to determine the effects of the intumescent coating parameters on the heat-blocking efficiency under different fire conditions.

2 Experiments

2.1 Laboratory Scale Fire Testing

The sample layout was designed to rapidly evaluate Intumescent fire retardants. Figure 1 depicts the laboratory setup to evaluate the performance of thin intumescent coatings in horizontal exposure to a methane torch. The image depicts a detailed illustration of a metal specimen exposed to heat. It provides the back view (A) and side view (B) for better understanding. The metal specimen is a square block with dimensions of 5” x 5” x 1/4” (127 mm x 127 mm x 6.3 mm). The front face of the steel block is coated with a 1-mm thick intumescent coating, which can be seen on the side view as an orange line.

A methane diffusion torch is positioned at varying distances from the metal specimen during the experiment to direct the flame onto the coating. The flame impact area on the coating surface is shown as a black line in Sketch B in Figure 1. Four thermocouple instruments (T1-T4) are used to measure the temperature at various points on the backside of the metal specimen. They are positioned with a vertical and horizontal spacing of 31 mm between them. Actual pictures of the experimental setup are shown in Figure 5 below. The methane torch can be seen on the right, heating the coating surface. The torch is clamped in position to maintain a constant distance to the coating surface. This will ensure a constant incidence heat flux to the surface. The red-hot area of the heated surface corresponding to the black line in Figure 1 can be clearly seen. On the left side, the four thermocouples can be seen drilled through a calcium silicate sample holder.

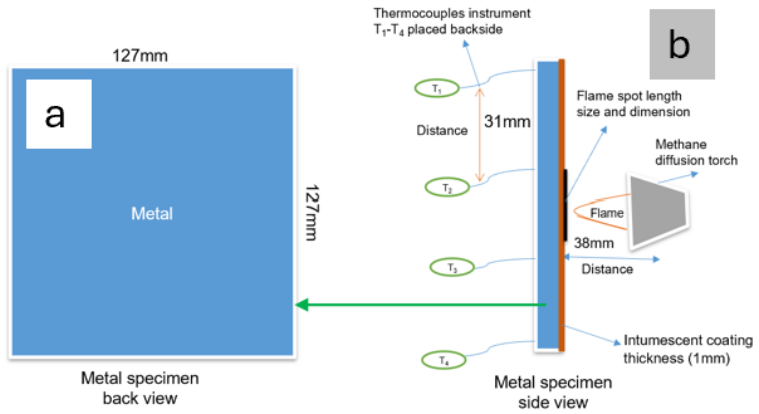

Figure 1. Laboratory Setup for Testing Intumescent Coatings Under Fire Conditions. a. metal specimen. b. positions of thermocouples attached to the back side of the steel plate.

2.1.1 Specimen preparation

An experimental method involves applying an epoxy-based intumescent coating onto a structural steel. Coatings were made by compounding Tannic Acid (Origin: Gall Nuts, Supplier: Sigma Aldrich), ammonium polyphosphate (Grade: AP422, Supplier Clariant) into a two-part epoxy system of EPON 828, and Ancamide 503. These components were combined at ratios detailed in Covello et al.7 and compounded with a spatula and vortex mixer until a uniform paste was observed. The coatings were applied to the substrate using a brush and pallet knife to achieve several coating thicknesses. The dry film thickness (DFT) was verified by an Elcometer DFT meter at 10 points on the plate. The prepared specimen with intumescent coating is illustrated in Figure 2. Thermal analysis samples were generated by exposing the intumescent films to the methane torch on this apparatus for various durations ranging from 0 to 60 minutes.

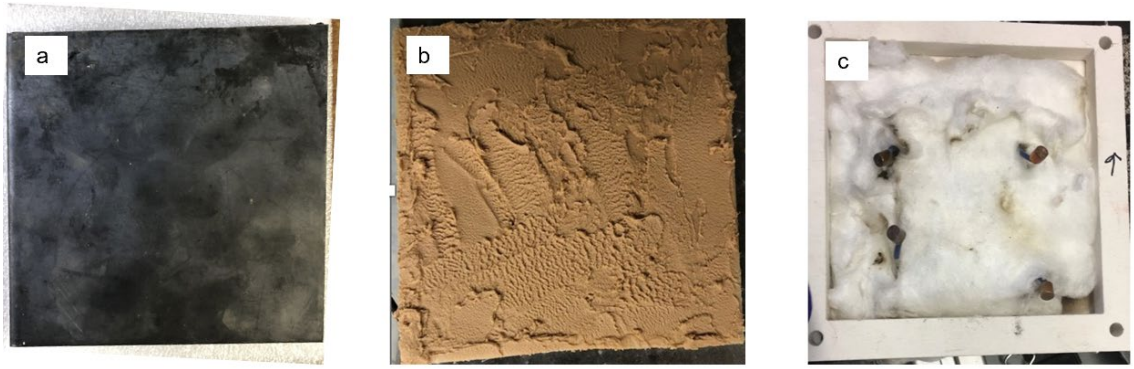

Figure 2. a. shows the steel substrate after being profiled before coating, b. shows the plate with a 1mm intumescent coating after curing, and c. shows the mineral wool placed inside the steel holder to minimize heat dissipation.

2.2 Water-cooled high heat flux sensor GG01

A GG01 water-cooled high heat flux sensor (Hukseflux Thermal Sensors), shown in Figure 3, was used to calibrate the methane torch and measure the heat flux emitted from the rear face at 1mm separation. The sensor was cooled with a 12.7 C water flow from the fume hood water supply. For calibration, the heat flux sensor was positioned at varying distances from 10 mm to 100 mm from the torch face, as can be seen in Figure 4. The resulting data points were then recorded and used as a calibration curve for the torch. A 40mm distance corresponding to a flux of 130 Kw/m^2 was selected and maintained for all discussed experiments.

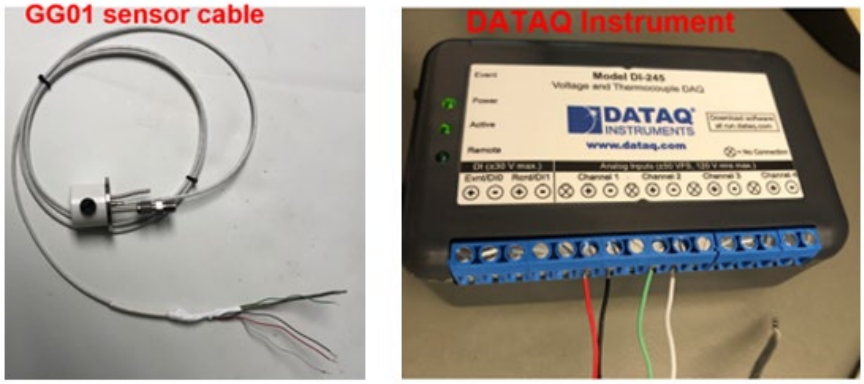

a b

Figure 3.a. Attaching GG01 sensor to, b. DATAQ Instruments for heat-flux measurement

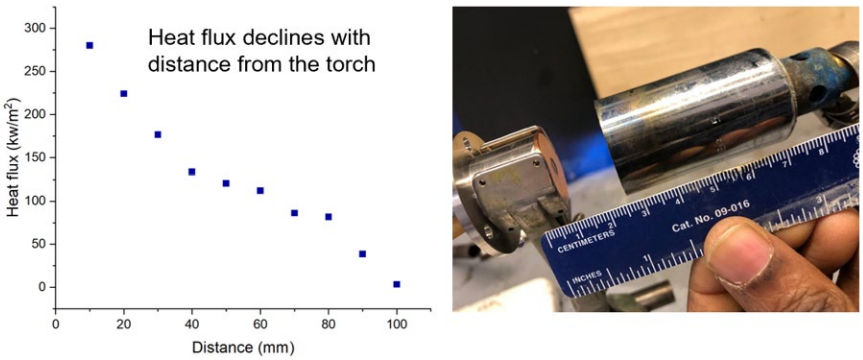

a b

Figure 4.a. Heat flux observed data as a function of torch distance, b. Measuring the distance between the torch and the coating surface.

2.3 TGA, DSC, and Density Experiments

2.3.1 Density

During the investigation, we used a Mettler Toledo XS205DU density balance (manufactured in the USA) to conduct density assessments. Anhydrous methanol from Sigma Aldrich (USA) was utilized as the immersion liquid to determine density. To ensure accuracy, we conducted three individual trials per sample and calculated the mean density value.

2.3.2 Modulated Differential Scanning Calorimetry (MDSC)

The epoxy-based intumescent coating samples were analysed using Differential Scanning Calorimetry (DSC) with a TA Instruments Q2000 differential scanning calorimeter. Samples were evaluated according to procedures described in (Making Accurate DSC and MDSC Specific Heat Capacity Measurements with the Q1000 Tzero DSC). Samples were first heated to a high temperature, then cooled in the DSC before modulation to measure reversing heat flow. The DSC was then programmed to modulated ± 1 C for a period of 100 s at various temperatures to collect heat flow data. This data was compared to a sapphire calibration standard for validity.

2.3.3 Thermogravimetric Analysis (TGA)

The epoxy-based coatings were tested for their mass-loss behaviours using Thermogravimetric Analysis (TGA) with a TA Instruments. The experiments were conducted at temperatures ranging from 50 to 800 C and were carried out using either laboratory-grade air or nitrogen at a flow rate of 50 mL/min. The heating rate was uniform at 10 C/min for all the experiments.

2.4 Methane diffusive torch experiments

Tests were conducted to evaluate the thermal resistance of epoxy-based intumescent coatings exposed to a flame source. The setup of methane torch is described in Section 2.1. A 3.8cm Meeker torch supplied with methane was used in this experiment. The heat flux used in the experiments was calibrated to 130 kW/m² at the centre of the dry film surface. The temperature at the coating surface and the underlying substrate were recorded throughout each test, which lasted for 20 minutes.

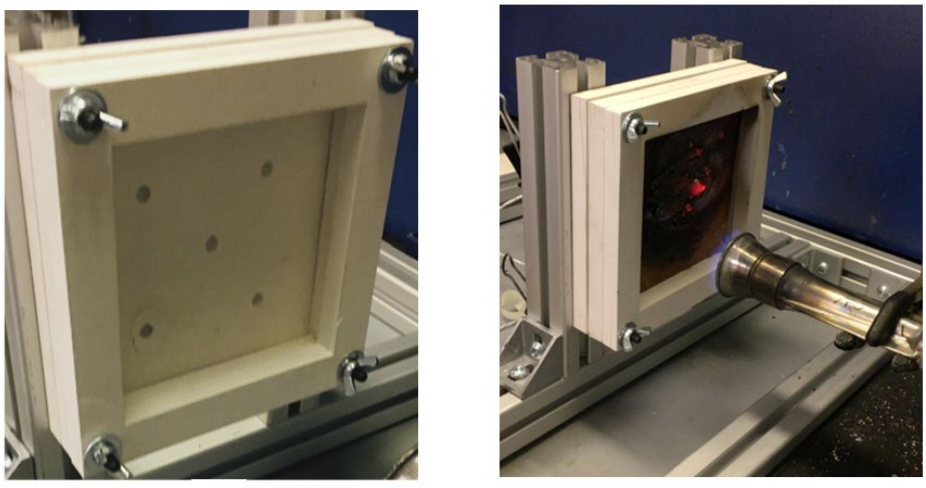

a b

Figure 5. a. Thermocouple array positioned equidistantly on steel's reverse side, b. Methane diffusion torch test on coated carbon steel

3 Numerical Simulation

The determination of the heat blocking efficient of intumescent coating using laboratory experiments could be challenging in both time and materially. Numerical simulations, especially finite element analyses, have been successful alternatives in overcoming these challenges. A well tested simulation can be used to augment our experiments in order to develop a meaningful result.

In this work, finite element simulations via the commercial software COMSOL Multiphysics 6.1 were used to mimic the experiment in estimating the heat flux and temperature distributions through the coating thickness. The equation for the heat transfer process is given in Equation 1, with the boundary conditions expressed in Equation 2. A complete or comprehensive analysis of the heat-blocking properties of the coating will need to examine the thermal conduction and expansion of the coating. This model could end up being complex and difficult since it will require thermal properties of both the coating matrix and the void as well as the dynamics of their formation, growth, and fusion. Since our coating is a new material, these properties are not readily available. To overcome this, we simulate only the heat transfer process as an effective heat transfer through the coating. The thermal properties of the intumescent coating are approximated with effective properties like the thermal conductivity, specific heat and density. The temperature-dependent thermal conductivity used in the simulation is given by Equation 3 and graphed in Figure 7. The density and specific heat were constant, 1190 kg/m^3 and 1470 J/kg-K respectively.

Therefore, the finite element analysis of the heating of a steel plate coated with a protective heat-blocking coating is formulated as in Equation 1. This equation represents the heat transfer in both the steel plate as well as the coating. The thermal properties k, ρ and cp are those for steel which we get from literature and listed in Table 1.

Table 1. Material characteristics and properties.

Symbols	Values	Unit	Descriptions	References
kcs	44.5	[W/m-K]	thermal conductivity	plotted based on the equation suggested by Çırpıcı, 2016 [33]
ρ_{CS}	7900	Kgm-3	Steel density	As quoted from the manufacturer (Metals Depot)
c_{CS}	475	Jkg-1K-1	Specific heat	Generated from a graph plotted based on the equation suggested by Çırpıcı, 2016 [33]

The corresponding properties for the coating are as explained above, the effective thermal conductivity, the effective specific heat and density.

$$\frac{\partial}{\partial x}\left(k\frac{\partial T}{\partial x}\right)+\frac{\partial}{\partial y}\left(k\frac{\partial T}{\partial y}\right)=\rho c_p\frac{\partial T}{\partial t} \quad (1)$$

Due to the symmetric nature of the heat transfer process, the three-dimensional process can be reduced to an equivalent two-dimensional problem. Actually, a one dimensional through the centre of the heated region will really suffice and greatly reduce the size of the finite element problem. A schematic representation of the domain of simulation together with the relevant boundary conditions are given in Figure 6.

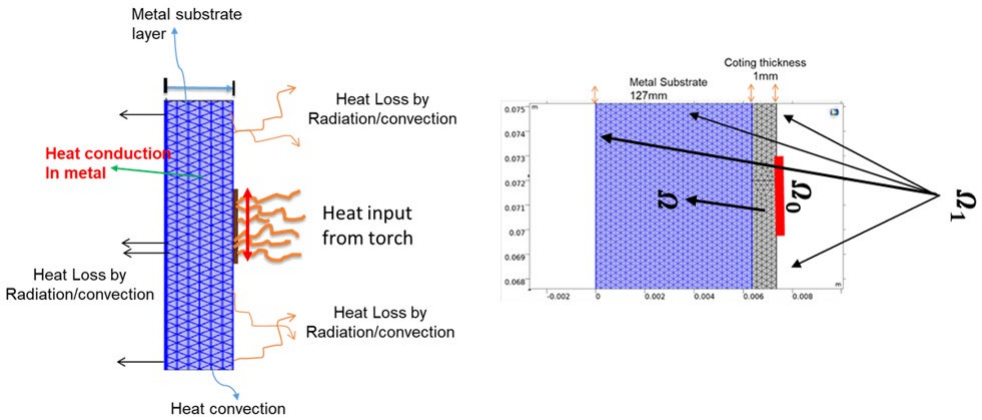

Figure 6. Schematic diagram of uncoated (Left) and coated (Right) substrate exposed to heat.

In Figure 6, the domain omega Ω comprises the through-thickness in the metal and coating. The heating torch is applied to the surface Ω_0 while all other exposed surfaces of the metal and coating, Ω_1, have heat loss to the ambient by convection and radiation. In the numerical method, these are all heat flux boundary conditions. Mathematically, these boundary conditions are expressed as Equations 2. and 3.

$$In\ heat\ flux\ from\ the\ torch - k\frac{\partial T}{\partial x} = q_0 \tag{2}$$

$$-k\frac{\partial T}{\partial x} = \underbrace{\varepsilon\sigma(T_{amb}^4 - T^4)}_{radiative} + \underbrace{h(T_\infty - T)}_{convective} \tag{3}$$

$$k_{coating} = \begin{cases} -2.9556 \cdot 10^{-4} \cdot T + 0.1552052 & T < 502℃ \\ 3.733595 \cdot 10^{-8} \cdot T^2 - 1.214936 \cdot 10^{-5} \cdot T + 3.966849 \cdot 10^{-3} & 502℃ \le T < 3000℃ \\ 0.1221 & T \le 3000℃ \end{cases} \tag{4}$$

The finite element analysis in COMSOL involves discretizing the domain in a mesh. The heat transfer process in the steel is well documented. The limiting domain in this work is the coating. We control the meshing of the computational domain by controlling the number of elements through the thickness of the coating. The default mesh sizes in COMSOL, extremely fine, normal, and extremely coarse, are used to test the sensitivity of the temperature solution to the mesh sizes. These are the default physics control mesh sizes in COMSOL. The extremely coarse mesh has 1 element through the coating thickness, normal mesh has 2 elements through the coating thickness, and extremely fine has 4 elements through the coating thickness. The result of the mesh sensitivity studies is given in Figure 8.a. The impact of mesh density on the simulated temperature profile is negligible, with a peak temperature of 397°C, 396°C, and 398°C for simulations with normal, extremely coarse, and extremely fine mesh densities, respectively. We control the number of elements through the thickness of the coating. To capture the temperature gradient through the coating thickness, we used 5 elements through the thickness of the coating which means for a 1 mm thick coating, the element size is 0.2 mm.

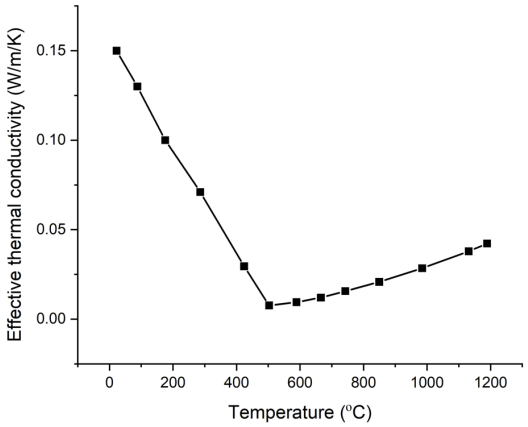

Figure 7. Effective thermal conductivity of the coating.

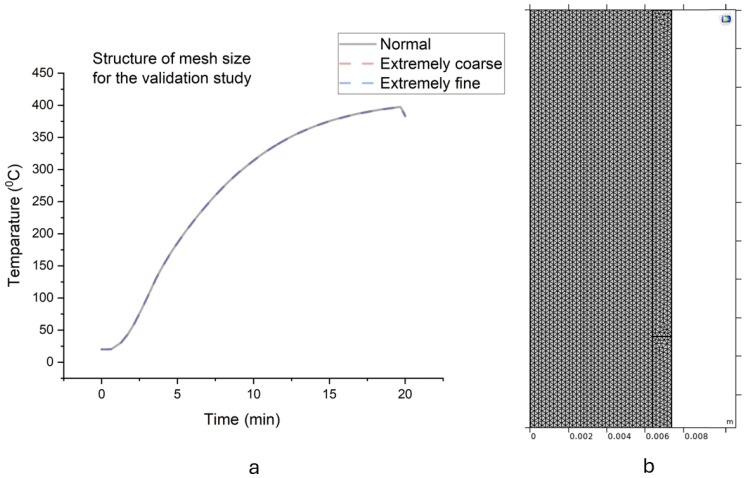

Figure 8.a. Metal-side temperature profile under various mesh conditions, b. Domain mesh that is used in the rest of the simulation.

4 Result and discussions

4.1 TGA Results

The TGA curve of the epoxy-based intumescent coating displays a mass loss pattern typical of such materials during thermal events. In Figure 9. The initial mass loss, noticeable from 100 to 150°C, with a subtle decline of 0.1%, is likely due to the evaporation of moisture or other volatile components. The curve remains relatively stable, no significant reaction is observed within the 150 to 220°C range. This suggests that the intumescent reaction may start at a higher temperature than what is typically reported. A significant mass loss occurs beyond 220°C, potentially indicating the onset of intumescence, which leads to the formation and stabilization of a char layer. The mass remains relatively constant until around 450°C, where the TGA curve begins to decrease, indicating the commencement of char degradation. This degradation continues until approximately 600°C. It is worth noting that the DTGA peak, which might suggest an exothermic oxidation reaction, does not correspond to a significant mass loss on the TGA curve. Therefore, the actual onset of thermal oxidation could be at a different temperature than the expected 405°C, requiring further analysis for precise determination.

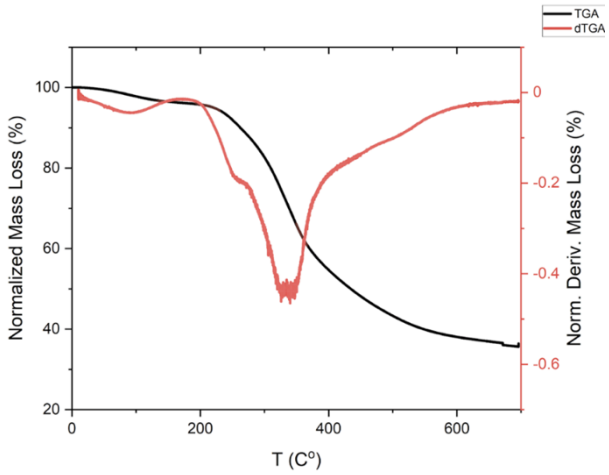

Figure 9. TGA plots Mass loss and rate of mass loss (DTG) for intumescent coatings heated under air.

4.2 DSC result

Figure 10 illustrates how the heat capacity of char changes with temperature. Below 200°C, there's a steady rise in heat capacity, followed by a decrease at higher temperatures around 300°C. This suggests that exothermic oxidation occurs in the char, leading to a reduction in its heat capacity.

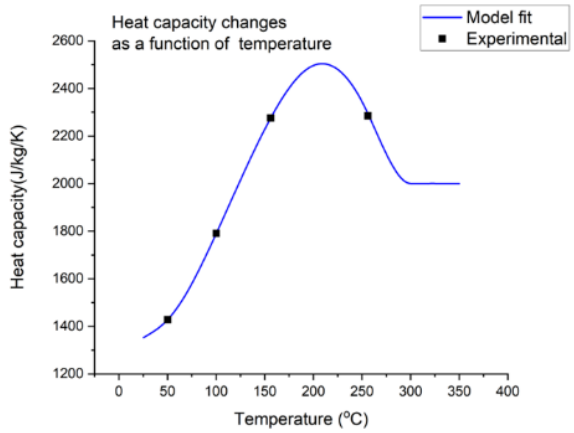

Figure 10. Variations in heat capacity with temperature: experimental results and model fits for intumescent coating.

4.3 Comparative analysis of thermal resistance

In Figure 11, we can observe a reduction in heat transfer. The intumescent coating surface temperature rises quickly, while the steel temperature remains below critical levels between 200 and 220°C. The model predictions were compared with experimental data. The surface temperature of the material ignited, causing it to rapidly climb to 530°C before dropping to between 500 and 490°C (as shown in Figure 11). The coating surface reached a steady temperature of between 500 and 520°C, depending on the coating expansion level. The coating surface's average temperature was measured experimentally using a thermal image camera, as depicted in Figure 12.

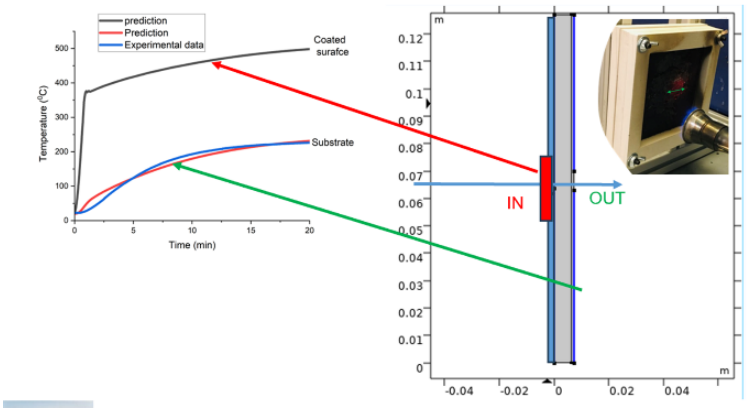

Figure 11. Comparison between the experimentally measured and numerical simulation for the coating surface and back of the steel temperature.

The coating's surface temperature changes were measured using a FLIR Thermovision A40 Infrared camera at a fixed distance from the steel plate's coated surface. The infrared thermography results showed temperature readings of around 580°C, which were recorded and analysed using the Research IR software suite. The recorded temperature matches the predicted temperature well.

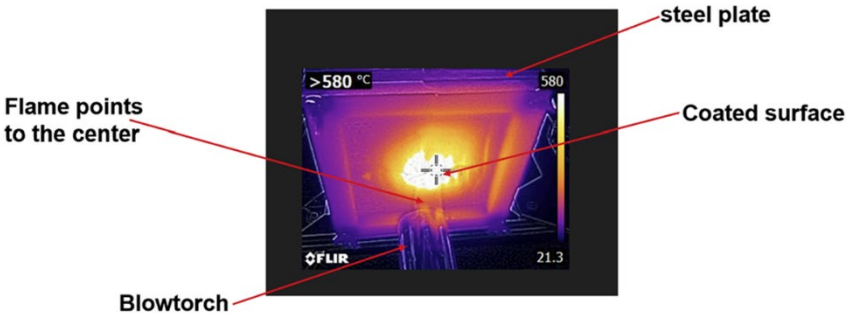

Figure 12. The infrared camera was positioned directly in front to capture the temperature of the front surface of the coated steel plate.

In Figure 13, the coating surface temperature predicted from the numerical simulation and experimental measurements is shown. The numerical simulations predicted the surface temperature fairly well.

The intumescent coating surface facing the methane torch is shown in Figure 14. The area circled in red is the region directly hit by the flame of the torch. The physical transformations, chemical reactions, and the significance of the intumescent coating's protective characteristics when subjected to heat are all examined. The char on the surface can affect both the surface heat flux and the thermal conductivity of the coating. In this numerical simulation, the effect of the coating is only accounted for the effective thermal conductivity of the intumescent coating. The char is not explicitly modelled. This effect will be examined in a later study.

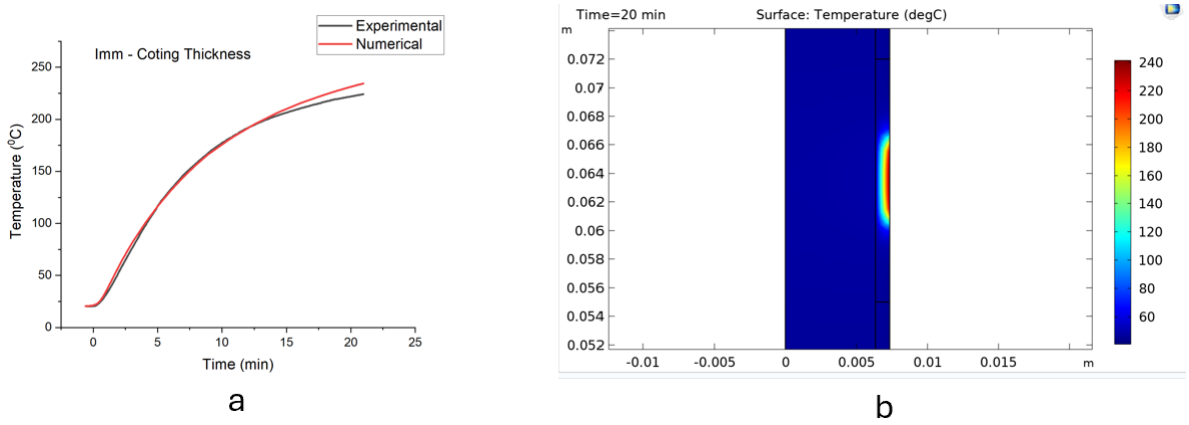

a b

Figure 13.a. Agreement in results between the simulation studies and experimental, and b. the thermal resistance of intumescent coatings-simulation.

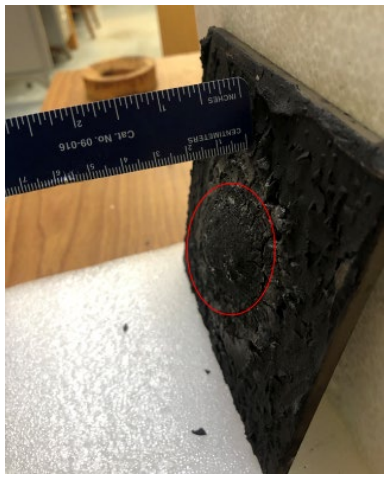

Figure 14. Photo of the specimen after exposure to methane diffusive torch test. The red circle highlights the area of direct flame impact.

4.4 Heat flux backside readings

The heat flux at the back surface of the metal specimen was also measured during the experiment. Figure 15 shows the water-cooled heat flux sensor used in measuring the heat flux, together with a comparison of the heat flux measurements for two coating materials, RSI-NMS and PAM E2. The heat flux measured from heating a bare steel plate is also shown in the graph as BLANK. It can be observed that the PAM-E2 coating does not provide any fire protection. The RSI-NMS coating provided a better protection of the steel surface.

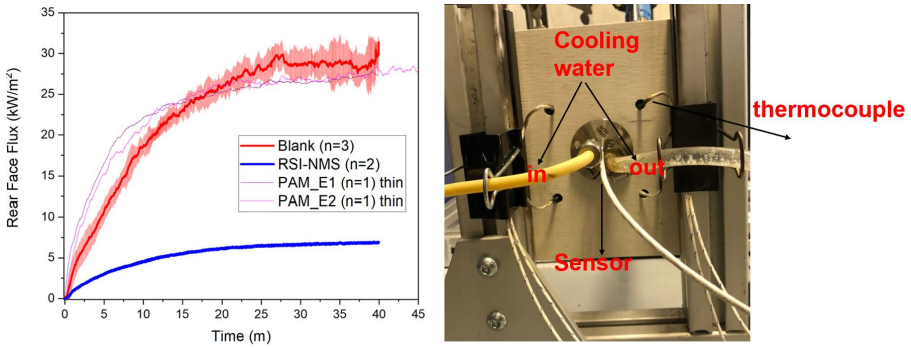

Figure 15. Evaluation of heat flux on the backside over time for uncoated and coated samples, Heat flux instrument experimental setups associated with testing.

From the good agreement obtained in the comparison of the numerical predictions and experimental measurements, numerical simulations were used to determine the heat-blocking efficiency of the 1 mm coating thickness with different flame exposure conditions (surface heat flux of 130, 68, and 35 Kw/m^2) to understand its effect on the heat-blocking efficiency. To that end, the different heat fluxes are applied at the coating surfaces to simulate the torch flame's application. The back of the steel plate has a radiative and convective boundary condition, as described above.

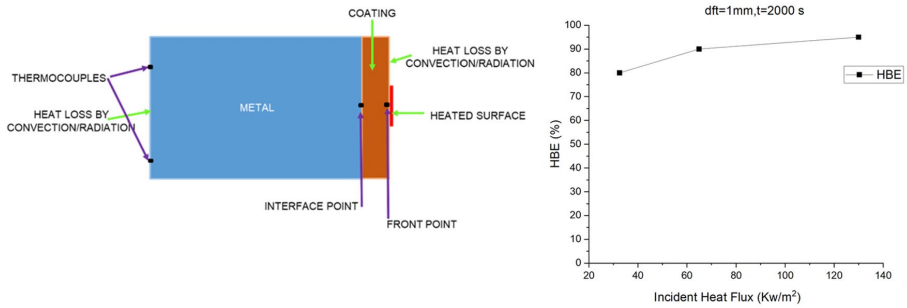

Figure 16. A 2-D heat transfer model simulates the heat transfer process in the metal-coating setting and the predicted heat-blocking efficiency

The heat-blocking efficiency (HBE) is determined according to the formula proposed by Kang et al. [19]

$$HBE = \left(1 + \frac{Transmitted\ heat\ flux}{Incident\ heat\ flux}\right) \times 100\% \quad (5)$$

The transmitted heat flux is calculated at a point in the steel just below the coated surface. The incident heat flux is the flux coming from the torch, which is the three applied heat fluxes discussed above. Figure 16 illustrates the modelling domain, showing the interface where the transmitted heat flux is recorded and the calculated HBE. The calculated HBE shows similar trends as in the Kang paper.

5 Conclusions

This research studied a mathematical model to estimate the thermal resistance and heat-blocking abilities of intumescent coatings against varying heat fluxes. It found that the efficiency of these coatings inversely relates to the heat flux intensity. The accuracy of material properties, mesh distribution in the simulation, and the application of boundary conditions are critical factors that specify the model's precision. Experimental evidence highlights the intumescent coatings' effectiveness in fire safety, suggesting they reliably predict and withstand actual fire scenarios.

Further improvements can be made by exploring the influence of fire-retardant additives, optimizing coating thickness, investigating different application methods, and assessing performance across various conditions and materials. Additional efforts should be directed toward improving the durability of coatings to withstand environmental impacts and enhancing the utilization of intumescent coatings for fire protection.

6 Acknowledgement

We thank the Saudi Cultural Mission (SACM) for their generous financial assistance through a full scholarship. This aid has enabled me to pursue my educational ambitions, and we sincerely appreciate their support. We thank the team at Case Western Reserve University's Sears Think [Box] for their valuable support in material design and fabrication and for engaging in productive discussions that greatly enhanced our project. We are also grateful to Underwriters Laboratories for supporting the CWRU combustion fire research laboratory, which has been essential to our research. I would like to express my sincere gratitude to Azizeh Amy Yousefi for her invaluable support and guidance throughout the course of this research. Her insightful suggestions and encouragement were instrumental in the completion of this work. Additionally, we would like to acknowledge Dr. Ankit Sharma for his insightful conversations that have contributed significantly to our understanding of the subject.

7 Nomenclature

The use of a nomenclature is non-mandatory, the possibility is also provided to explain every notation and symbol right after their occurrence in text. Please either include a nomenclature here, just before the reference section, or explain every notation and symbol one-by-one.

$\boldsymbol{q_0}$	Heat source / Heat flow / heat flux
ε	Surface factor or Front face emissivity
σ	Stefan–Boltzmann constant
h	Convection coefficient
T_∞	Temperature outside the body
T	Temperature of the body surface
T_{amb}^4	Ambient temperature

8 References

[1] S. Sun, Q. Yu, B. Yu, and F. Zhou, “New Progress in the Application of Flame-Retardant Modified Epoxy Resins and Fire-Retardant Coatings,” *Coatings*, vol. 13, no. 10, p. 1663, 2023.

[2] A. Lucherini, “Fundamentals of thin intumescent coatings for the design of fire-safe structures,” 2020.

[3] J. Zhang, L. Huang, T. Chen, and G. Su, “Simulation based analysis of electrical fire risks caused by poor electric contact between plug and receptacle,” *Fire Saf. J.*, vol. 126, p. 103434, 2021.

[4] B. K. Kandola and A. R. Horrocks, “Flame retardant composites, a review: the potential use of intumescents,” *Spec. Publ.-R. Soc. Chem.*, vol. 224, pp. 395–420, 1998.

[5] J. H. Beh, “Development of fire-protective water-borne intumescent coating incorporated with rubberwood ash for steel,” UTAR, 2022.

[6] K. Mróz, I. Hager, and K. Korniejenko, “Material solutions for passive fire protection of buildings and structures and their performances testing,” *Procedia Eng.*, vol. 151, pp. 284–291, 2016.

[7] E. J. Price, J. Covello, A. Tuchler, and G. E. Wnek, “Intumescent, epoxy-based flame-retardant coatings based on poly (acrylic acid) compositions,” *ACS Appl. Mater. Interfaces*, vol. 12, no. 16, pp. 18997–19005, 2020.

[8] O. Zybina and M. Gravit, “Basic Ingredients of Intumescent Compositions,” in *Intumescent Coatings for Fire Protection of Building Structures and Materials*, Springer, 2020, pp. 1–51.

[9] M. M. de Souza, S. C. de Sa, A. V. Zmozinski, R. S. Peres, and C. A. Ferreira, “Biomass as the carbon source in intumescent coatings for steel protection against fire,” *Ind. Eng. Chem. Res.*, vol. 55, no. 46, pp. 11961–11969, 2016.

[10] G. Wang and J. Yang, “Influences of binder on fire protection and anticorrosion properties of intumescent fire resistive coating for steel structure,” *Surf. Coat. Technol.*, vol. 204, no. 8, pp. 1186–1192, 2010.

[11] F. Takahashi, “Fire blanket and intumescent coating materials for failure resistance,” *MRS Bull.*, vol. 46, no. 5, pp. 429–434, 2021.

[12] Y. Yan, S. Dong, H. Jiang, B. Hou, Z. Wang, and C. Jin, “Efficient and durable flame-retardant coatings on wood fabricated by chitosan, graphene oxide, and ammonium polyphosphate ternary complexes via a layer-by-layer self-assembly approach,” *ACS Omega*, vol. 7, no. 33, pp. 29369–29379, 2022.

[13] B. K. Cirpici, Y. C. Wang, and B. Rogers, “Assessment of the thermal conductivity of intumescent coatings in fire,” *Fire Saf. J.*, vol. 81, pp. 74–84, 2016.

[14] Y. Zeng, C. E. Weinell, K. Dam-Johansen, L. Ring, and S. Kiil, “Effects of coating ingredients on the thermal properties and morphological structures of hydrocarbon intumescent coating chars,” *Prog. Org. Coat.*, vol. 143, p. 105626, 2020.

[15] A. Lucherini, J. P. Hidalgo, J. L. Torero, and C. Maluk, “Influence of heating conditions and initial thickness on the effectiveness of thin intumescent coatings,” *Fire Saf. J.*, vol. 120, p. 103078, 2021.

[16] A. H. Ridoy, M. R. Molla, A. Chakrobarty, and M. I. Kayes, “A Finite Element Method Investigation of Mechanical and Thermal Behavior of Composite Coatings on Steel Bar.”.

[17] Z. Wang, F. Jia, E. R. Galea, and J. Ewer, “Computational fluid dynamics simulation of a post-crash aircraft fire test,” *J. Aircr.*, vol. 50, no. 1, pp. 164–175, 2013.

[18] B. K. Cirpici and I. Aydin, “Investigation of Intumescent Coating on the Fire Endurance of Concrete-Filled Steel Columns with Varied Characteristics,” *J. Mater. Res. Technol.*, 2023.

[19] J. Kang, F. Takahashi, and J. S. T’ien, “In situ thermal-conductivity measurements and morphological characterization of intumescent coatings for fire protection,” *J. Fire Sci.*, vol. 36, no. 5, pp. 419–437, 2018.

[20] F. Bozzoli, A. Mocerino, S. Rainieri, and P. Vocale, “Inverse heat transfer modeling applied to the estimation of the apparent thermal conductivity of an intumescent fire retardant paint,” *Exp. Therm. Fluid Sci.*, vol. 90, pp. 143–152, Jan. 2018, doi: 10.1016/j.expthermflusci.2017.09.006.

[21] J. Han, G.-Q. Li, Y. C. Wang, and Q. Xu, “An experimental study to assess the feasibility of a three stage thermal conductivity model for intumescent coatings in large space fires,” *Fire Saf. J.*, vol. 109, p. 102860, 2019, doi: https://doi.org/10.1016/j.firesaf.2019.102860.

[22] Y. Zhang, Y. C. Wang, C. G. Bailey, and A. P. Taylor, “Global modelling of fire protection performance of intumescent coating under different cone calorimeter heating conditions,” *Fire Saf. J.*, vol. 50, pp. 51–62, May 2012, doi: 10.1016/j.firesaf.2012.02.004.

[23] “Rusthi et al. - 2017 - Investigating the fire performance of LSF wall sys.pdf.”

[24] H.-C. Huang and A. S. Usmani, *Finite Element Analysis for Heat Transfer*. London: Springer London, 1994. doi: 10.1007/978-1-4471-2091-9.

[25] B. K. Çırpıcı, S. N. Orhan, and T. Kotan, “Numerical modelling of heat transfer through protected composite structural members,” *Chall. J. Struct. Mech.*, vol. 5, no. 3, p. 96, Sep. 2019, doi: 10.20528/cjsmec.2019.03.003.

[26] T. A. Burkhart, D. M. Andrews, and C. E. Dunning, “Finite element modeling mesh quality, energy balance and validation methods: A review with recommendations associated with the modeling of bone tissue,” *J. Biomech.*, vol. 46, no. 9, pp. 1477–1488, 2013.

[27] J. X. Wen, K. Kang, T. Donchev, and J. M. Karwatzki, “Validation of FDS for the prediction of medium-scale pool fires,” *Fire Saf. J.*, vol. 42, no. 2, pp. 127–138, 2007.

[28] A. Borg and O. Njå, “The concept of validation in performance-based fire safety engineering,” *Saf. Sci.*, vol. 52, pp. 57–64, 2013.

[29] M. Bundy, A. Hamins, J. Gross, W. Grosshandler, and L. Choe, “Structural fire experimental capabilities at the NIST National Fire Research Laboratory,” *Fire Technol.*, vol. 52, pp. 959–966, 2016.

[30] S. L. Manzello, T. Cleary, J. Shields, and J. Yang, “Building and Fire Research Laboratory (BFRL) National Institute of Standards and Technology (NIST) Gaithersburg, MD 20899-8662 1Official contribution of the National Institute of Standards and Technology, not subject to copyright in the United”.

[31] A. Tewarson, W. Chin, and R. Shuford, “Materials specifications, standards, and testing,” *Handb. Build. Mater. Fire Prot.*, p. 1, 2004.

[32] L. Choe and J. Gross, “Introducing a new structural-fire testing capability at NIST and large-scale structural-fire experiments,” 2017.

[33] B. K. Cirpici, Y. C. Wang, B. D. Rogers, and S. Bourbigot, “A theoretical model for quantifying expansion of intumescent coating under different heating conditions,” *Polym. Eng. Sci.*, vol. 56, no. 7, pp. 798–809, Jul. 2016, doi: 10.1002/pen.24308.

[34] M. R. D. Silveira, R. S. Peres, V. F. Moritz, and C. A. Ferreira, “Intumescent Coatings Based on Tannins for Fire Protection,” *Mater. Res.*, vol. 22, no. 2, p. e20180433, 2019, doi: 10.1590/1980-5373-mr-2018-0433.